Journal of Instrumentation

Initial trials of a dose monitoring detector for boron neutron capture therapy

Published by IOP Publishing for Sissa Medialab

Received: *October 21, 2020*
Accepted: *November 28, 2020*
Published: *January 22, 2021*

Initial trials of a dose monitoring detector for boron neutron capture therapy

T.A. Bykov,[a,b] **D.A. Kasatov,**[a,b] **A.M. Koshkarev,**[a,b] **A.N. Makarov,**[a,b] **V.V. Porosev,**[a,1] **G.A. Savinov,**[a] **I.M. Shchudlo,**[a,b] **S.Yu. Taskaev**[a,b] **and G.D. Verkhovod**[a,b]

[a] *Budker Institute of Nuclear Physics, Lavrentiev ave. 11, Novosibirsk 630090, Russia*
[b] *Novosibirsk State University, Pirogova st. 2, Novosibirsk 630090, Russia*

E-mail: porosev@inp.nsk.su

Abstract: In this study, we present results of initial trials of a scintillator-over-fiber detector system with a silicon photomultiplier readout designed at Budker Institute of Nuclear Physics. The results demonstrate that the proposed system, using a pair of boron-enriched and boron-free scintillators, could be successfully used for monitoring of thermal neutron flux and estimation of irradiation dose. Nevertheless, it is necessary to optimize the design of the detector head components to ensure long time detector stability with heavy radiation background.

Keywords: Dosimetry concepts and apparatus; Neutron detectors (cold, thermal, fast neutrons); Photon detectors for UV, visible and IR photons (solid-state) (PIN diodes, APDs, Si-PMTs, G-APDs, CCDs, EBCCDs, EMCCDs, CMOS imagers, etc); Scintillators, scintillation and light emission processes (solid, gas and liquid scintillators)

[1] Corresponding author.

https://doi.org/10.1088/1748-0221/16/01/P01024

2021 JINST 16 P01024

Contents

2021 JINST 16 P01024

1 Introduction

At present, accelerator-based neutron sources are considered as the best choice for pre-clinical and clinical studies for boron neutron capture therapy (BNCT) [1]. For this goal, a proton tandem accelerator with a lithium neutron-producing target was developed at BINP [2, 3]. A much higher intensity of neutron source in comparison with reactor-based ones requires an adequate dose-monitoring system to verify treatment procedures. Therefore, we designed a multichannel scintillator-over-fiber detector system with a silicon photo-multiplier (SiPM) readout [4]. Simultaneous application of two different registration channels: the first one, sensitive to gamma radiation, and the second one, sensitive to gamma radiation and neutrons, allows us to estimate the contribution of the neutron component more accurately. A similar approach was developed in Japan [5, 6]. Using SiPMs instead of vacuum photo-multipliers made it possible to implement a detection system with much higher efficiency and a larger number of detector channels. In the detector we used polystyrene-based plastic scintillators: SC-331 enriched with boron, and SC-301, without boron, which were designed in the early 2000s at the Institute for High-Energy Physics (IHEP, Protvino) [7]. They have a fast response of ~ 2.5 ns and, by specifications, use the same fluors (p-terphenyl, POPOP). In addition, the scintillator SC-331 contains 0.9% of natural isotope of Boron-10. Because of significantly higher concentration of Boron-10 in the scintillator material in comparison with patient tissues where it is $\sim$5–50 ppm [8], the detector itself will absorb much higher doses during treatment, $\sim$ 1–10 kGy. Therefore, evaluation of stability of detector components becomes a vital issue.

2 Design of sensors

The sensitive element of the detector is a cylinder with diameter of 1 mm and length of 1 mm made of plastic scintillator. It is placed inside of a light-reflecting cylinder made of hard Teflon with wall thickness of 1 mm. The top side of the scintillator is painted with custom-made MgO-based white paint. The scintillator is glued to a plastic optical fiber (POF) with epoxy, and all components are placed inside of a black plastic case. Two sensors, one with a boron enriched scintillator and a boron-free one, are combined in one detector head. The design of the detector head is schematically shown in figure 1.

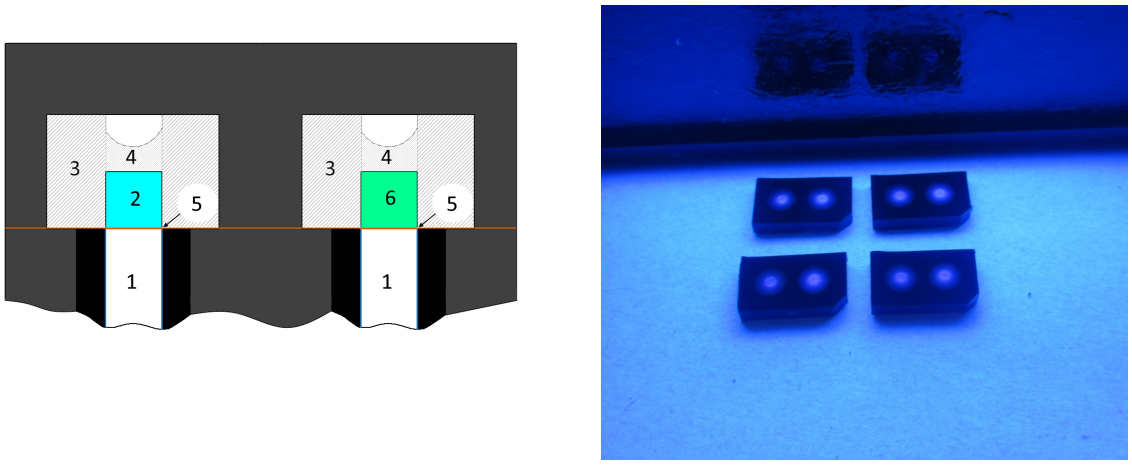

Figure 1. General design of detector head (left) and photo of assembled sensors under UV light (right). 1- POF, 2- boron-enriched scintillator, 3- hard Teflon, 4- white reflective paint, 5- epoxy, 6- conventional scintillator.

The absorption of a neutron by ^{10}B in a boron enriched scintillator produces with a 94% probability an excited ^{7}Li nucleus, which de-excites with the emission of 478 keV gamma quantum. The emitted gamma rays could be detected in the boron-less scintillator and produce an extra signal. To estimate a relative signal value in two detector channels, we performed a Monte-Carlo simulation using the 'GEANT4' simulation package. Neutrons with the energy of 0.1 eV were directed into a boron enriched scintillator, and we accumulated a total value of optical photons detected by SiPMs in both registration channels in one run. In each run, 10^5 primary neutrons were generated.

Figure 2 represents the relative intensity of the signals in detector channels as a function of the distance between the sensors. Additionally, data for different POF lengths are presented.

Despite the closeness of two detector elements to each other, the magnitude of a signal induced in the gamma detector by photons generated in a capture reaction in the neutron detector is approximately 10^{-5} and can be regarded as negligible.

2021 JINST 16 P01024

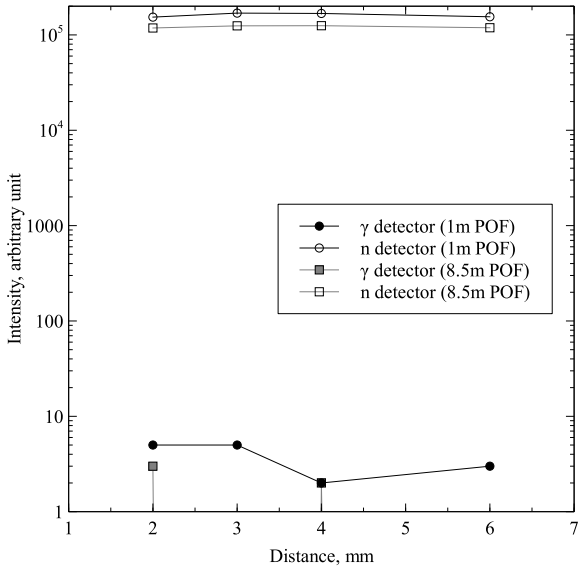

Figure 2. Relative signal intensities in detector channels when the boron enriched scintillator is irradiated with neutrons.

3 Material studies

Because of concentration of Boron-10 in the scintillator and heavy gamma background from the neutron-generating target and surrounding materials, the scintillator and other detector components will absorb high doses during treatment. To evaluate that we performed a series of material aging tests using an industrial electron accelerator ILU-10 (BINP, Novosibirsk) at a fixed irradiation dose of 15 kGy [9].

3.1 Emission spectrum of the scintillator

To measure the emission spectrum of a scintillator, it was excited with an ultraviolet (UV) light-emitting diode (UVTOP300-HL-TO39, ROITHNER LASERTECHNIK GmbH)[1] with a wavelength of 305 nm, near the maximum of photo-absorption of the primary fluorophore. The fluorescence spectrum of the scintillator was measured by the method of light transmission through a sample 1 mm thick. The spectral data were accrued on a stand based on a monochromator MDR-12U (LOMO, St.Petersburg), equipped with a photo-diode C10439-03 (HAMAMATSU). Since the data were measured using a monochromator with a diffraction grating, the true spectrum was restored using the dependence of the reflection coefficient on the wavelength, known from the grid data sheet, and the photodiode spectral sensetivity data.

Figure 3 shows emission spectra of the SC-301 scintillator sample before and after irradiation. As with other plastic scintillators, the shape of emission spectrum has not significantly changed at this dose level [10].

[1] http://www.roithner-laser.com.

2021 JINST 16 P01024

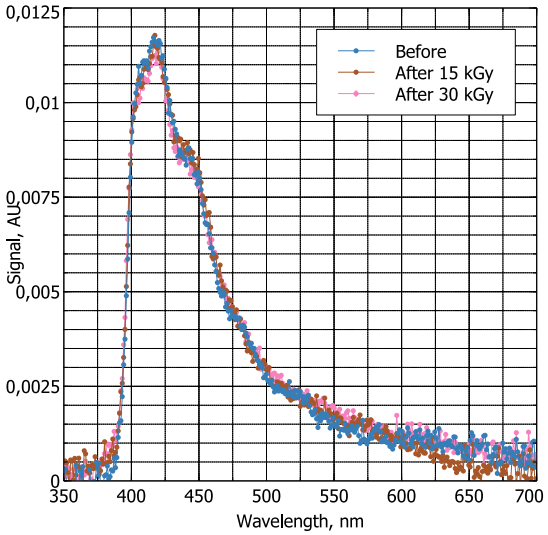

Figure 3. Scintillator emission spectra before and after irradiation.

3.2 Epoxy studies

To select an optimal optically transparent epoxy for detector assembling, we performed a comparison study of several optical epoxy glues produced in Russia[2] and a few other ones. General views of the samples before and just after irradiation are shown in figure 4.

Figure 4. Epoxy samples before and just after irradiation. 1- PEO-510KE-20/0 , 2- PEO-610KE-20/0, 3- PEO-210KE, 4- PEO-490KE, 5-PEO-490ME, 6- POLYTEC EP610, 7- BICRON BC-600.

Figure 5 demonstrates the light transmission as a function of the wavelength for the samples before and just after irradiation.

The epoxies PEO-490KE and PEO-490ME demonstrated good radiation hardness. Unfortunately, they have a rather high recommended curing temperature of 110–120°C and therefore they could not be generally used with plastic scintillators. All other samples showed significant deterioration in parameters, with the exception of PEO-210, which was used in further experiments.

[2] http://www.lfpti.ru/english.htm.

2021 JINST 16 P01024

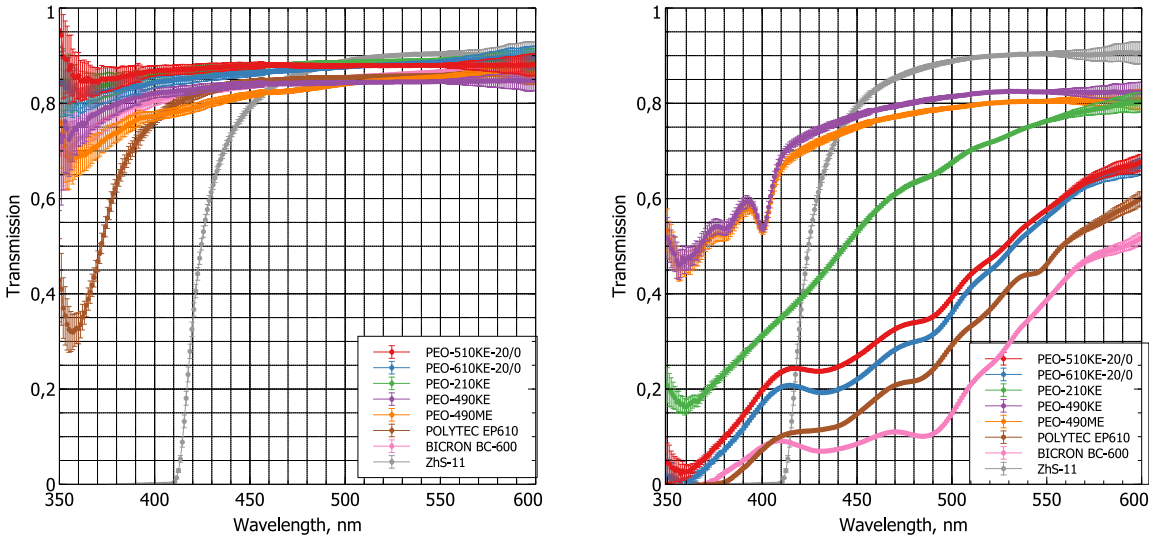

Figure 5. Light transmission through the samples before (left) and after (right) irradiation. For a reference, data for an optical filter ZhS-11 are presented too.

3.3 Light transmission of POF

The light transmission of the POFs was measured at the same stand that was used to measure the emission spectra of scintillators. The initial spectral intensity of a light source with halogen lamps (LOMO PHOTONICA) was measured with a small fragment of optical fiber 10 cm long. Figure 5 demonstrates the light transmission through ASAHI SB-1000 fibers 1 m and 8.5 m long as a function of the wavelength. Unirradiated fibers demonstrate the absorption bands of carbon bonds in polymethylmethacrylate (PMMA) [11].

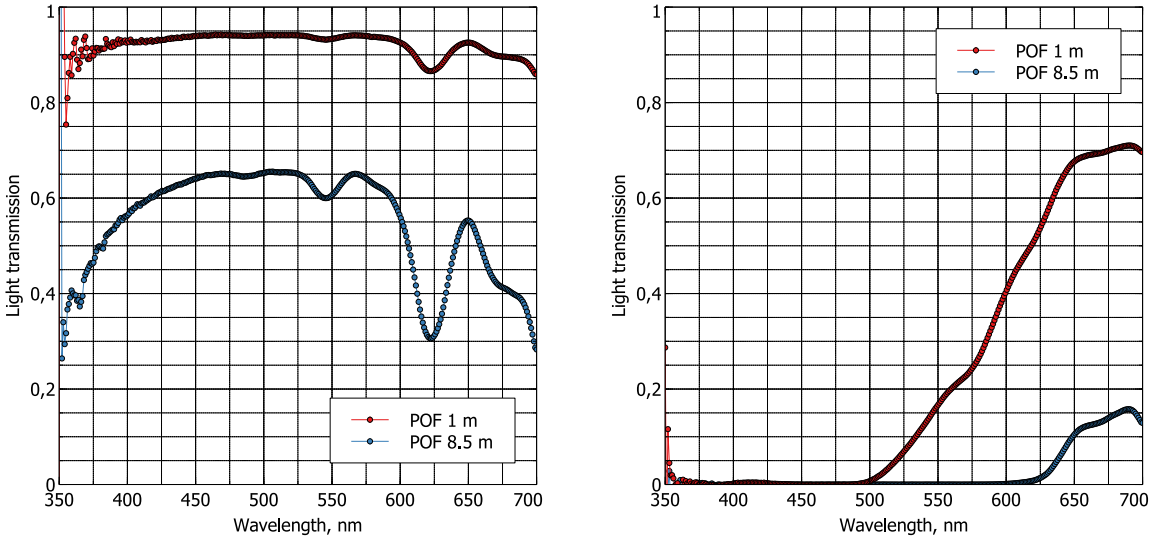

Figure 6. Light transmission through POF samples before (left) and after (right) irradiation.

After exposure to radiation from the accelerator, the optical fibers showed dramatic degradation of transparency, especially at wavelengths corresponding to the maximum of the scintillator emission spectrum. Therefore, we can expect signal reduction due to the POF aging in real operation.

4 Detector signals

The degradation of light transmission in the detector components under radiation leads to signal drop on the photo-detector. For the tests, the detector heads were assembled with plastic optical fiber ASAHI SB-1000 of a length of 8.5 m. MPPC S13360-3050CS (HAMAMATSU) was used as the photo-detector. In the readout electronics unit, two EASIROC ASICs [12] were connected in parallel to ensure the possibility of counting the same events with different independent thresholds. Each EASIROC channel includes an 8-bit DAC, a variable gain preamplifier, and a fast shaper (15 ns), followed by a discriminator with an adjusted threshold. The data were continuously accumulated in 5 ms intervals and sent to the computer for further processing. During the operation, the control software measures the environmental temperature and adjusts the bias voltage to keep the SiPM gain constant.

To evaluate stability of signal magnitude, we measured the detector counts as a function of the discriminator threshold in the beginning and after a few test sessions with neutrons. In this period, the total proton charge on the neutron generating target exceeds ~ 150 C. Results at the beginning of the test session are shown in figure 7 and at the end of the session, in figure 8. Figure 7 (right) and figure 8(right) demonstrate the difference in the signals of neutron+gamma sensitive channels and corresponding gamma sensitive ones. During the experiments, we used three different detector heads, which could be placed in different positions relative to the neutron-generating target. It explains the observed signal difference between the detectors. Generally, signals from the boron-enriched scintillator demonstrate significant excess of counts, which is related to detection of neutrons.

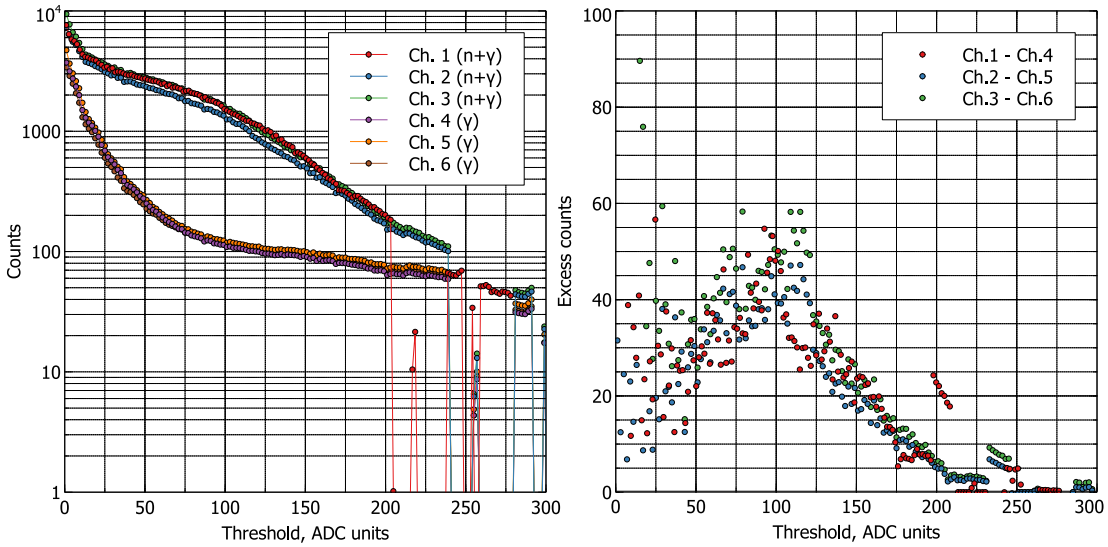

Figure 7. Counts versus threshold (left) and signal difference between neutron+gamma sensitive and gamma sensitive channels (right). Initial trials.

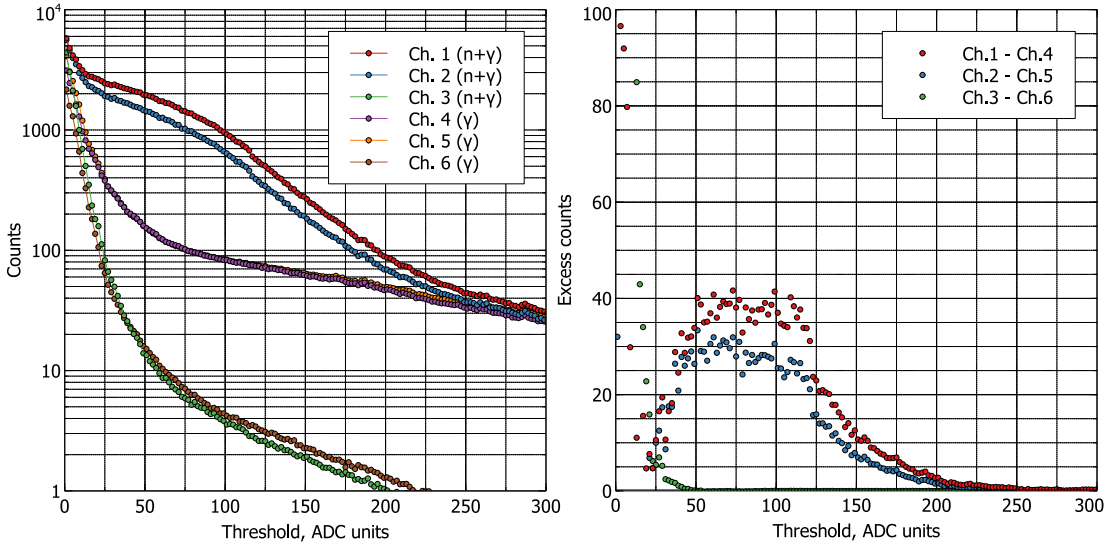

Figure 8. Counts versus threshold (left) and signal difference between neutron+gamma sensitive and gamma sensitive channels (right). Total charge on neutron-generating target is ~ 150C.

Under irradiation, the spectrum of neutron related events shifts towards lower amplitudes. In routine operation, we used a detection threshold of ~ 50 ADC units to reduce the contribution of the SiPM noise and the Cherenkov light generated in the POFs. Therefore, the degradation of optical components leads to losses of neutron-related events. Finally, figure 9 demonstrates the same spectra after a rather long period of use of the detector heads. In this case, the total charge on the neutron generating target exceeded ~ 356 C.

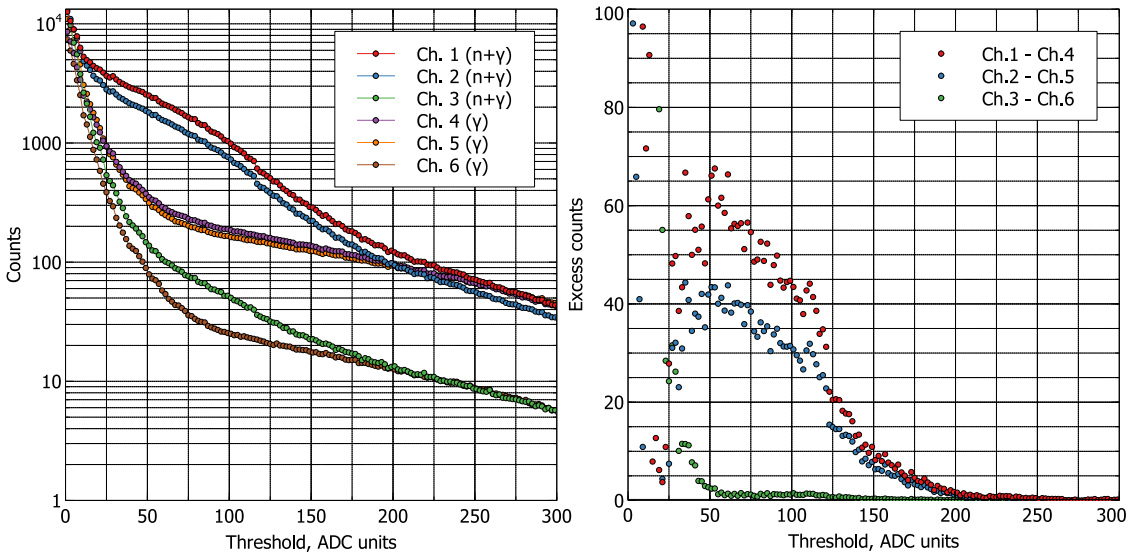

Figure 9. Counts versus threshold (left) and signal difference between neutron+gamma sensitive and gamma sensitive channels (right). Total charge on neutron-generating target is ~ 356 C.

2021 JINST 16 P01024

The observed spectra clearly demonstrate degradation of the sensors. At that time we disassembled one detector head and measured the light transmission through its optical fibers. Figure 10 shows the light transmission as a function of the wavelength.

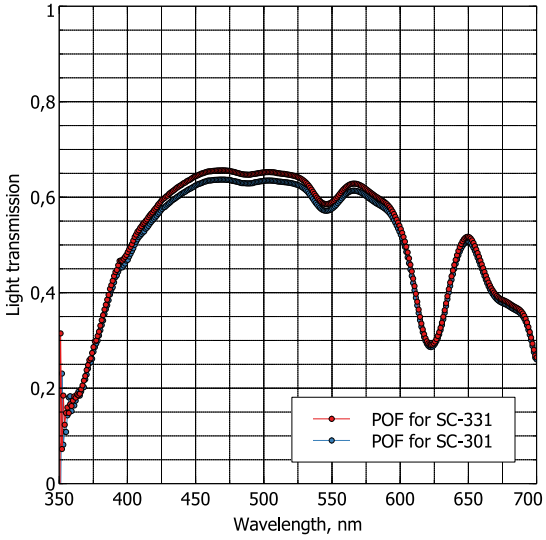

Figure 10. Light transmission through sensor POFs. Total charge on neutron-generating target is ~ 356 C.

One can see that both fibers exhibit practically identical light attenuation in the range of 350–450 nm. One possible solution of this problem is using specially designed quartz optical fibers of low activation materials, which could be superior than the POFs [13]. Another way is employing scintillators with the position of the maximum in the fluorescence spectrum in the range of 450–500 nm or wavelength-shifters.

5 Results and discussion

On the accelerator neutron source of BINP, experiments are underway to study the effect of neutron radiation on cell cultures and laboratory animals to further develop the BNCT technique. During research [14–16], the absorbed dose was determined only by numerical simulation of the transport of neutrons and gamma radiation [17, 18]. Now it is possible to use the developed neutron detector to measure and control the "boron" dose caused by the reaction $^{10}B(n,\alpha)^{7}Li$, which provides the main contribution to the absorbed dose.

At the accelerator, a stationary proton beam with an energy of 2.1 MeV, current of up to 3 mA, and transverse size of 3 cm hits on a neutron-generating target. The target is made in the form of a copper disk 8 mm thick with channels for water cooling. A 60 µm-thick lithium layer of 82 mm in diameter is deposited onto the copper disk. The copper disc is pressed against an aluminum base with a cooling water inlet and outlet pipes. As a result of the $^{7}Li(p,n)^{7}Be$ threshold reaction, neutrons with an average energy of 108 keV are generated [19].

To slow down the neutrons, a moderator made of PMMA with thickness of 7.2 cm and diameter of 20 cm is used. Generally, cell cultures are placed in flasks under the moderator on the surface of a phantom with diameter of 20 cm and height of 24 cm made of PMMA too. Figure 11 shows

2021 JINST 16 P01024

graphs of the spatial distribution of the "boron" dose rate for different layouts. The "boron" dose was calculated from the counting rate of the detector, assuming a boron-10 content of 40 ppm in the cell cultures.

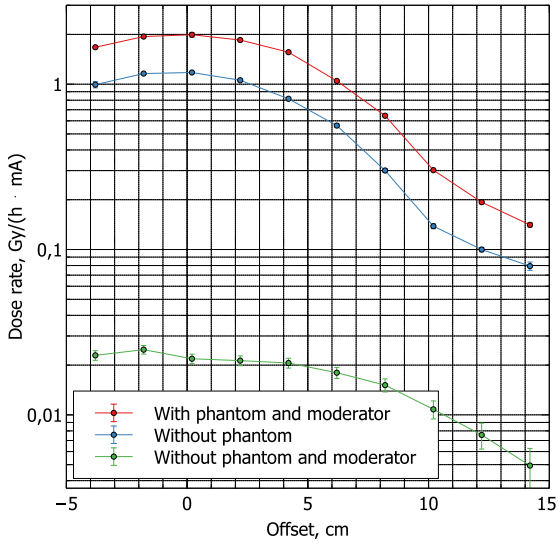

Figure 11. Dose rate versus distance to beam axis.

It is seen that the generated neutron flux is rather uniform and is characterized by a high boron dose rate of up to 2 Gy/(h · mA). The figure also shows that if the phantom is removed, the dose rate drops 1.7 times. This indicates that the phantom returns some of the neutrons to the studied area, further slowing them down. If we remove the moderator too, the dose rate is further reduced ~ 50 times. It confirms the fact that accelerator-based neutron sources generate epithermal neutrons mainly.

Thus, the developed detector becomes a tool for monitoring the "boron" dose during irradiation and an instrument for optimization and verification of the neutron beam formation system.

6 Conclusion

In this study, we presented results of initial trials of a scintillator-over-fiber detector system with a silicon photo-multiplier readout. The results demonstrate that the proposed system could be successfully used for monitoring of thermal neutron flux. Anyway, there are several issues to address to ensure reliable operation of the detector. In particular, it is necessary to optimize the design of detector head components to provide better signal-noise separation and to ensure long time stability of detector parameters.

Acknowledgments

The research is partially supported by a grant of the Russian Science Foundation (project No. 19-72-30005).

2021 JINST 16 P01024

References

[1] Y. Kiyanagi, *Accelerator-based neutron source for boron neutron capture therapy*, *Ther. Radiol. Oncol.* **2** (2018) 55.

[2] D. Kasatov et al., *The accelerator neutron source for boron neutron capture therapy*, *J. Phys. Conf. Ser.* **769** (2016) 012064.

[3] S.Y. Taskaev, *Accelerator based epithermal neutron source*, *Phys. Part. Nucl.* **46** (2015) 956

[4] T.A. Bykov et al., *A multichannel neutron flux monitoring system for a boron neutron capture therapy facility*, 2019 *JINST* **14** P12002

[5] M. Ishikawa et al., *Early clinical experience utilizing scintillator with optical fiber (SOF) detector in clinical boron neutron capture therapy: Its issues and solutions*, *Radiat. Oncol.* **11** (2016) 105.

[6] M. Ishikawa et al., *Development of real-time thermal neutron monitor using boron-loaded plastic scintillator with optical fiber for boron neutron capture therapy*, *Appl. Radiat. Isot.* **61** (2004) 775.

[7] I.G. Britvich et al., *New Polystyrene-Based Scintillators*, *Instrum. Exp. Tech.* **45** (2002) 644.

[8] K. Hideghety et al., *Tissue uptake of BSH in patients with glioblastoma in the EORTC 11961 phase I BNCT trial*, *J. Neurooncol.* **62** (2003) 145.

[9] V. Auslender et al., *Electron Accelerator for Energy up to 5.0 MeV and Beam Power up to 50 kW with X-ray Converter*, in *Proceedings of EPAC 2004*, Lucerne Switzerland (2004), https://accelconf.web.cern.ch/e04/PAPERS/THPKF050.PDF.

[10] L. Zhao et al., *Properties of plastic scintillators after irradiation*, *Nucl. Instrum. Meth. A* **552** (2005) 449.

[11] O. Ziemann, J. Krauser, P.E. Zamzow and W. Daum, *POF handbook: Optical short range transmission systems*, Springer, Heidelberg Germany (2008).

[12] S. Callier, C.D. Taille, G. Martin-Chassard and L. Raux, *EASIROC, an Easy & Versatile ReadOut Device for SiPM*, *Phys. Procedia* **37** (2012) 1569.

[13] T. Nakamura et al., *Characteristics of Radiation-Resistant Real-Time Neutron Monitor for Accelerator-Based BNCT*, *J. Radiat. Protect. Res.* **41** (2016) 105.

[14] A. Zaboronok et al., *Boron-neutron capture therapy in Russia: preclinical evaluation of efficacy and perspectives of its application in neurooncology*, *New Armen. Med. J.* **11** (2017) 1.

[15] E. Sato et al., *Radiobiological response of U251MG, CHO-K1 and V79 cell lines to accelerator-based boron neutron capture therapy*, *J. Radiat. Res.* **59** (2018) 101.

[16] E. Zavjalov et al., *Accelerator-based boron neutron capture therapy for malignant glioma: a pilot neutron irradiation study using boron phenylalanine, sodium borocaptate and liposomal borocaptate with a heterotopic U87 glioblastoma model in SCID mice*, *Int. J. Radiat. Biol.* **96** (2020) 868.

[17] L. Zaidi et al., *Neutron-Beam-Shaping Assembly for Boron Neutron-Capture Therapy*, *Phys. Atom. Nuclei* **80** (2017) 60.

[18] L. Zaidi et al., *Beam Shaping Assembly Design of $^7Li(p,n)^7Be$ Neutron Source for Boron Neutron Capture Therapy of Deep-seated Tumor*, *Appl. Radiat. Isot.* **139** (2018) 316.

[19] C.L. Lee and X.-L. Zhou, *Thick target neutron yields for the $^7Li(p,n)^7Be$ reaction near threshold*, *Nucl. Instrum. Meth. B* **152** (1999) 1.

2021 JINST 16 P01024